

Background Debiased SAR Target Recognition via Causal Interventional Regularizer

Hongwei Dong^{a,b,*}, Fangzhou Han^{c,*}, Lingyu Si^{a,b}, Wenwen Qiang^{a,b},
Lamei Zhang^c

^a*Science & Technology on Integrated Information System Laboratory, Institute of Software, Chinese Academy of Sciences, Beijing, China*

^b*University of Chinese Academy of Sciences, Beijing, China*

^c*Department of Information Engineering, Harbin Institute of Technology, Harbin, China*

Abstract

Recent studies have utilized deep learning (DL) techniques to automatically extract features from synthetic aperture radar (SAR) images, which shows great promise for enhancing the performance of SAR automatic target recognition (ATR). However, our research reveals a previously overlooked issue: SAR images to be recognized include not only the foreground (i.e., the target), but also a certain size of the background area. When a DL-model is trained exclusively on foreground data, its recognition performance is significantly superior to a model trained on original data that includes both foreground and background. This suggests that the presence of background impedes the ability of the DL-model to learn additional semantic information about the target. To address this issue, we construct a structural causal model (SCM) that incorporates the background as a confounder. Based on the constructed SCM, we propose a causal intervention based regularization method to eliminate the negative impact of background on feature semantic

*Equal Contributions

learning and achieve background debiased SAR-ATR. The proposed causal interventional regularizer can be integrated into any existing DL-based SAR-ATR models to mitigate the impact of background interference on the feature extraction and recognition accuracy. Experimental results on the Moving and Stationary Target Acquisition and Recognition (MSTAR) dataset indicate that the proposed method can enhance the efficiency of existing DL-based methods in a plug-and-play manner.

Keywords: Deep learning, Causal inference, Synthetic aperture radar, Automatic target recognition, Background debias

1. Introduction

Synthetic aperture radar (SAR) is an active remote sensor that enables all-weather and day-and-night detection, making it a crucial component of Earth observation systems (Moreira et al., 2013). One of the primary objectives of SAR image data processing is automatic target recognition (ATR) (El-Darymli et al., 2016). Achieving this goal requires automated and intelligent methods that can accurately recognize targets by extracting discriminative features from SAR images, which remains a challenging task (Kechagias-Stamatis and Aouf, 2021).

Deep learning (DL) overcomes the limitations of traditional manual feature engineering and delivers superior performance in a data-driven manner, making it a powerful solution to address the aforementioned challenge (LeCun et al., 2015). Researchers have made initial forays into DL-based SAR-ATR methods in recent years (Chen et al., 2016), but further refinement is necessary before they can be effectively applied to real-world scenarios due

to their relatively short development time (Zhu et al., 2021).

The general structure of SAR-ATR systems consists of three phases: detection, discrimination, and recognition. In related studies, the first two phases, commonly known as the focus-of-attention (FOA), are employed to locate the region of interest (ROI) that may contain targets, without necessitating any human intervention. Both traditional (El-Darymli et al., 2013) and DL-based approaches (Zou et al., 2022) have demonstrated satisfactory FOA performance.

Using the results of FOA as input, the SAR-ATR method is designed to infer the classes of targets that may be included in the ROI. In this phase, the discriminability of extracted features (i.e., the feature with larger inter-class distance and smaller intra-class distance is more discriminative) is crucial for recognition performance. Various traditional methods have been proposed to improve the feature discriminability, such as hand-crafted feature extractors (Amrani et al., 2018), attributed scattering centers (Li and Du, 2019), low-rank matrix factorization (Zhang et al., 2018). However, DL-based methods offer substantial advantages in terms of performance compared to traditional approaches. Chen et al. (2016) and Ding et al. (2016) conduct pioneering work that utilize DL-models for SAR image feature extraction and target recognition, setting the foundation for further advancements. Subsequently, a significant portion of research has focused on refining the model architecture to enhance the performance of SAR-ATR, including multi-stream (Pei et al., 2017), attention mechanism (Zhang et al., 2020), capsule structure (Ren et al., 2021), vision transformer (Wang et al., 2022), etc. Given that SAR image processing often encounters the issue of speckle noise, some stud-

ies have proposed methods for extracting the speckle-noise-invariant features (Kwak et al., 2019; Lei et al., 2021). Another aspect of the research focuses on adversarial learning, which involves using generative models for data augmentation (Sun et al., 2019) or performing adversarial attacks on existing models (Peng et al., 2022; Du and Zhang, 2021) to enhance the robustness of their feature extraction. In addition, research on DL-based methods for environments with a limited number of training samples (Fu et al., 2022; Wen et al., 2021) and edge devices (Wang et al., 2021) is gradually emerging.

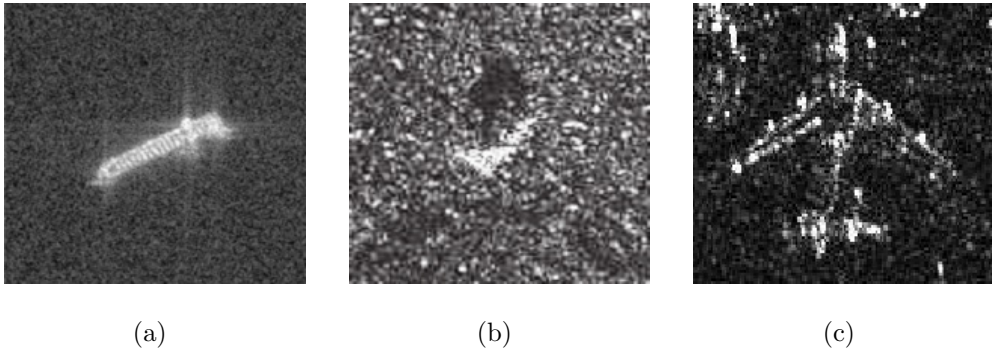


Figure 1: Typical targets in SAR images. (a) Ship target (Huang et al., 2018). (b) Vehicle target (AFRL and DARPA, 2020). (c) Aircraft target (Sun et al., 2022).

The aforementioned studies have advanced the capability of SAR-ATR from a methodological perspective, but have overlooked the issue of background interference. As shown in Fig. 1, the ROI includes not only the foreground (i.e., target), but also a certain size of the background. Therefore, the following question arises:

- *When the foreground and background of two SAR images are different, do the DL-model extracted features belong to the foreground, the*

background, or a mixture of both?

A satisfactory answer to this question is that the DL-model extracts semantic information solely from the foreground, as the background is irrelevant for target recognition. In this way, the discriminability of extracted features can be maximized. However, in reality, the situation may differ. Firstly, it should be noted that eliminating the background in ROI can be challenging due to the irregular shape and non-standardized size of non-cooperative targets (Huang et al., 2018; AFRL and DARPA, 2020; Sun et al., 2022). Therefore, the input of SAR-ATR typically includes both foreground and background. Then, we conduct a motivating experiment to demonstrate that the features extracted by DL-models are a mixture of foreground and background elements.

Specifically, we employ two DL-based models, i.e., VGG16 (Simonyan and Zisserman, 2014) and ResNet18 (He et al., 2016), and evaluate their performance on the Moving and Stationary Target Acquisition and Recognition (MSTAR) dataset (AFRL and DARPA, 2020). This dataset is constructed for scientific research purposes and contains only cooperative vehicle targets that possess similar sizes, roughly measuring 40×40 . Based on this observation, we evaluate the performance of two DL-models under four distinct crop conditions: preserving only the central 40×40 , 64×64 , 88×88 , and 128×128 image crops, while masking the remaining areas. The accuracy and feature visualizations of different experimental setups are shown in Fig. 2.

As shown in Fig. 2(a), the accuracy of SAR-ATR progressively decreases as the image background intensifies. Moreover, Fig. 2(b)-(d) demonstrate that the inclusion of background reduces the distance between dif-

ferent classes in the latent space, thereby diminishing the discriminability

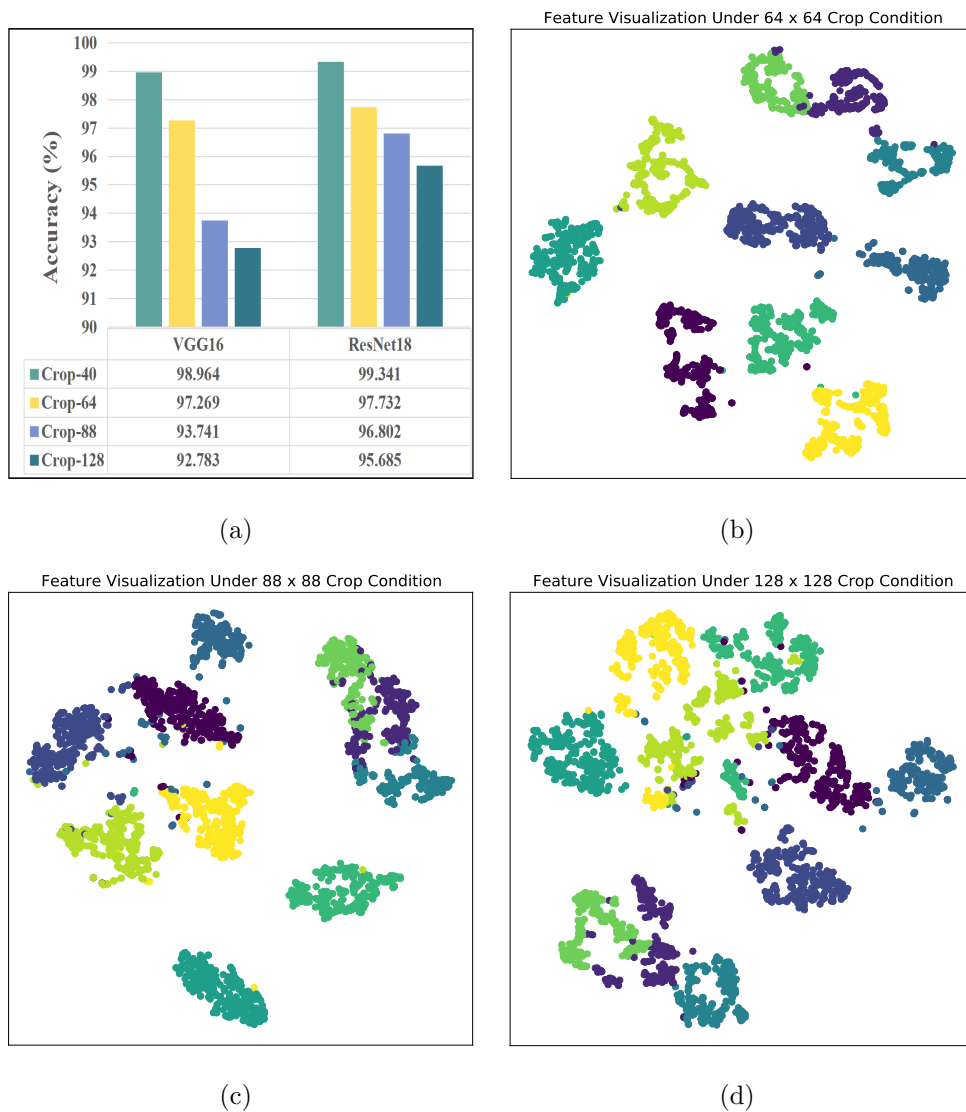


Figure 2: Results of the motivating experiment for four image crop methods. (a) Recognition accuracy of different center-crops. (b)-(c) Feature visualization of 64×64 , 88×88 and 128×128 center-crops using t-SNE (Van der Maaten and Hinton, 2008).

of extracted features. This phenomenon is reasonable from a causal perspective since there is no semantic correlation between the foreground and background. Therefore, the elements belonging to the background in the extracted features cannot have a positive impact on target recognition. Both the experimental and theoretical analyses indicate that the background is likely to interfere with the feature extraction process, which should focus on the foreground, leading to biased feature learning objectives and the deterioration of feature quality.

To address this issue, we utilize a structural causal model (SCM) (Pearl, 2009) to depict the causal relationships among the variables in the SAR-ATR process, including the input, DL-model, foreground, background, and prediction. In the proposed SCM, the background is set as the confounder, which is consistent with the motivating experimental results. By analyzing this SCM, we obtain a theoretical solution for treating background interference. This guides us to represent the theoretical background elimination process as a causal interventional regularizer. As a result, we can achieve background debiased feature learning, support better feature discriminability, and subsequently obtain satisfactory SAR-ATR performance. In summary, the main contributions of this paper are three-fold:

- (1) We highlight a critical but overlooked issue that the background exerts an adverse influence on the performance of SAR-ATR, and offer a remedy based on the perspective of causal inference.
- (2) We construct a SCM based on the process of SAR image feature learning to depict the causal relationships among the input, DL-model, foreground, background, and prediction. This provides a theoretical expla-

nation and solution for background interference.

- (3) Guided by the constructed SCM, we propose a causal intervention based regularization method. This method can be utilized to effectively mitigate the adverse effects of background on feature learning of the DL-model in a plug-and-play manner, leading to significant enhancement in the performance of SAR-ATR.

The remainder of this paper is organized as follows. Section 2 briefly reviews related works. Section 3 describes the proposed method. Experiment results and analyses are presented in Section 4. Finally, Section 5 concludes this paper.

2. Related Works

This section provides a comprehensive review of the research literature related to this paper, including DL-based SAR-ATR methods, background related methods, and causality theory.

2.1. General Paradigm of DL-based SAR-ATR

Convolutional neural network (CNN) is one of the most significant DL techniques and has achieved state-of-the-art results in various image processing applications, particularly image recognition. The fundamental prototype of CNN, proposed by [LeCun et al. \(1989\)](#), is characterized by desirable properties such as weight sharing and local connection. [Krizhevsky et al. \(2012\)](#) have made significant contributions to the development of current CNN models by using ReLU activation, local response normalization, and GPU training to enhance model capacity and efficiency. CNN is typically regarded as an

end-to-end methodology for feature extraction and classification, providing automated feature engineering that is more powerful than traditional hand-crafted features and kernel methods.

The seminal studies of DL-based SAR-ATR method are conducted by [Chen et al. \(2016\)](#) and [Ding et al. \(2016\)](#). These studies utilize stacked CNN models composed of convolution, activation, pooling, and fully-connected layers to extract abstract but discriminative deep features from SAR images to achieve promising performance in target recognition. Despite considerable research in this area and some progress being made, the background debiased DL-based SAR-ATR approach has not been explored so far, which is the objective of this paper.

2.2. Background Debias Related Studies in SAR-ATR

Several studies have analyzed the effect of background on SAR-ATR ([Pappson and Narayanan, 2012](#); [Cui et al., 2005](#); [Lombardo et al., 2001](#)). Empirical evidence provides by [Zhou et al. \(2019\)](#) demonstrates the significant impact of background replacement on the performance of SAR-ATR. Moreover, [Belloni et al. \(2020\)](#) discuss the role of target, shadow, and clutter in recognition to gain insight into the decision-making process of DL-models.

While there is currently no research exploring background bias from a methodological perspective, the impact of this issue has been observed in the implementation of many SAR-ATR methods. In related studies, the negative effects caused by the background are mitigated by employing two main techniques, i.e., image pre-processing and data augmentation. The image pre-processing method ([Feng et al., 2022](#)) involves a multi-stage algorithm that begins by detecting the edges of the target, allowing for the segmen-

tation of the target region from the background. Then, chip recognition is performed to improve performance. On the other hand, the data augmentation method (Ding et al., 2016; Chen et al., 2016) is based on sampling a large number of chips from the original image with the same foreground but slightly different backgrounds. These operations prompt the DL-model to learn background-irrelevant features.

However, both of the techniques mentioned above have obvious drawbacks: Firstly, the image pre-processing method not only risks losing target details but also has a high level of complexity. Secondly, the data augmentation method relies on a strong prior, i.e., all targets to be recognized have a fixed and known size. This approach can be challenging when dealing with the recognition problem of non-cooperative targets. In this paper, we address this issue from a causal inference perspective and propose an end-to-end method with a plug-and-play capability.

2.3. Causality Theory

Causality has become as a significant subfield of statistics, with its own conceptual framework, descriptive language, and methodological system. A comprehensive review of the existing literature in (Schölkopf, 2022) highlights how causality theory has been instrumental in the development of machine learning by addressing the deficiencies of current approaches.

SCM (Pearl, 2009) is a crucial tool in causality theory as it can effectively depict the interdependencies between factors involved in a process using a graph structure. By scrutinizing the SCM, every conceivable alteration that may take place within a process and the pluralistic consequences arising from these alterations may be identified. With the help of SCM, the distinction

between correlation and causality can be explored, leading to the current causal inference framework (Glymour et al., 2016). This framework decomposes the problem into three levels: correlation, intervention, and counterfactual, corresponding to observation, action, and imagination, respectively. Intervention, which involves altering part of the variable generation mechanism while preserving the remainder, is a critical operation for determining and quantifying causality. Scientific research commonly employs intervention, such as through randomized controlled experiments, to establish the presence and direction of causality.

3. Methodology

This section presents a detailed introduction to the proposed method for causal intervention based regularization. First, we introduce the construction and analyses of the SAR-ATR oriented SCM. Next, we provide a comprehensive overview of the proposed method, including its model architecture and loss function.

In contrast to many variants in this field that prioritize model refinement, the proposed method focuses on a background debiased feature learning process. This approach eliminates interference from the background in DL-based SAR-ATR models, guided by causal intervention. This process significantly enhances the discriminability of the extracted features and resulting in superior recognition performance.

3.1. Causal Analysis

To illustrate the impact of background in the process of SAR-ATR, we use the SCM as a basis for our analysis. The SCM is a directed acyclic graph in

which nodes represent variables and directed edges indicate causality between them.

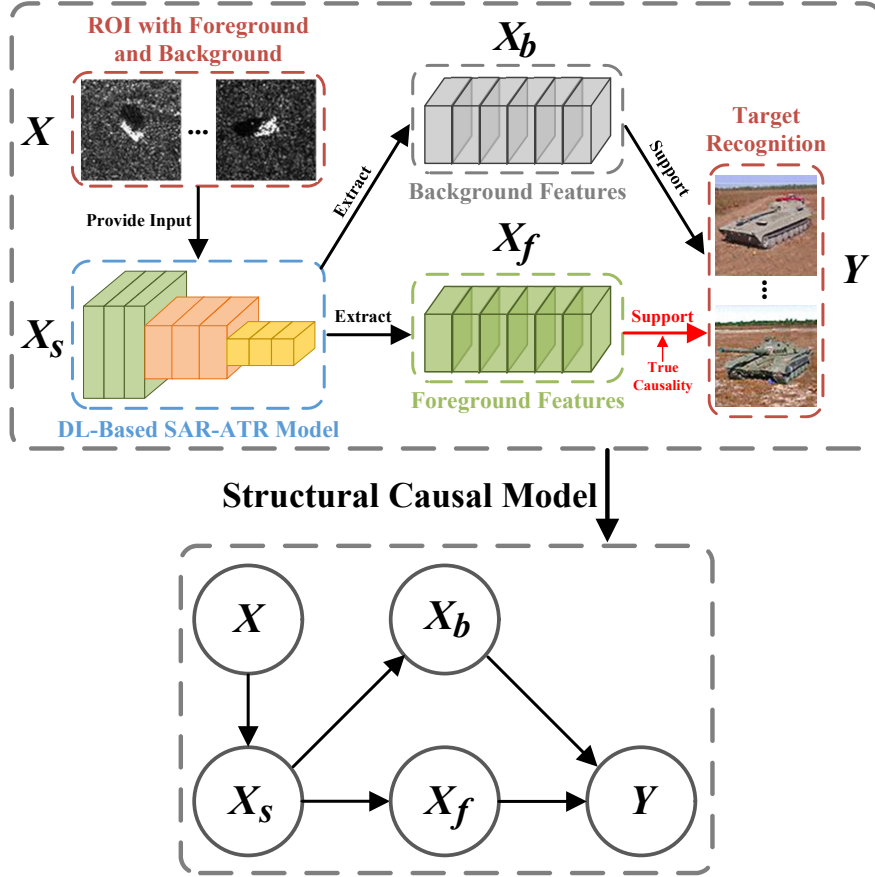


Figure 3: Illustration of the constructed SCM. It depicts the causal relationships among the variables in the SAR-ATR process, including the input, DL-model, foreground, background, and prediction. The top part uses examples to demonstrate the conceptual causality. The bottom part is the abstracted SCM for DL-based SAR-ATR.

As shown in Fig. 3, we refer to the input SAR images as X , the feature extractor of the DL-based SAR-ATR model as X_s , and the features extracted by X_s as $(X_f; X_b)$, where X_f corresponds to foreground features

and \mathbf{X}_b corresponds to background features. The recognition of the label \mathbf{Y} is supported by both \mathbf{X}_f and \mathbf{X}_b . In the following, we provide a detailed description of the proposed SCM and the underlying principles behind its construction.

$\mathbf{X} \rightarrow \mathbf{X}_s$ indicates that the DL-model \mathbf{X}_s is used to extract features from the input SAR images \mathbf{X} . $\mathbf{X}_s \rightarrow \mathbf{X}_b$ indicates that background features \mathbf{X}_b is extracted by the model \mathbf{X}_s . $\mathbf{X}_s \rightarrow \mathbf{X}_f$ indicates that \mathbf{X}_f is extracted by \mathbf{X}_s . $\mathbf{X}_b \rightarrow \mathbf{Y}$: This link indicates that recognition of input SAR images relies on the information in the background features \mathbf{X}_b , since all DL-model extracted features are used for the prediction of \mathbf{Y} . $\mathbf{X}_f \rightarrow \mathbf{Y}$: This link represents that the label of an input sample is determined by its foreground features, which is the true causality.

As previously analyzed, the ideal DL-model should capture the true causality between \mathbf{X}_f and \mathbf{Y} . Therefore, we expect the prediction of the input SAR image to be driven primarily by the foreground features, rather than the background features. However, as shown in the constructed SCM, the conventional DL-model fails to capture such causality because the prediction \mathbf{Y} is not only determined by \mathbf{X}_f via the link $\mathbf{X}_f \rightarrow \mathbf{Y}$, but also by the spurious correlation via the link $\mathbf{X}_f \leftarrow \mathbf{X}_s \rightarrow \mathbf{X}_b \rightarrow \mathbf{Y}$. It means that the DL-based feature extractor \mathbf{X}_s generates the background features \mathbf{X}_b from the background of \mathbf{X} . These features provide part of the semantics that are utilized when recognizing targets.

The above causalities can be reflected in the motivating experiment corresponding to Fig. 2: The performance of DL-based SAR-ATR models trained on input SAR images that include both foreground and background is signif-

icantly lower compared to models trained on background-removed data. To capture the true causality while suppressing the spurious correlation, we perform backdoor adjustment by intervening on \mathbf{X}_f using the $do(\cdot)$ operation. This allows us to express the causality between \mathbf{X}_f and \mathbf{Y} as $P(\mathbf{Y}|do(\mathbf{X}_f))$, rather than relying on $P(\mathbf{Y}|\mathbf{X}_f)$.

It is widely recognized that the channels of the extracted features from any DL-based feature extractor are closely related to the underlying feature semantics (Zhou et al., 2016). Then we can simply assume that the output of the last network layer of \mathbf{X}_s , i.e., $(\mathbf{X}_f; \mathbf{X}_b)$, can be mapped into a series of feature semantics, denoted as $(\mathbf{X}_f; \mathbf{X}_b) \mapsto \{F_i\}_{i=1}^n$, where $F_i \in \mathbb{R}^{n_c}$ represents a stratification of feature semantics. Considering that the confounder \mathbf{X}_b is contained in $(\mathbf{X}_f; \mathbf{X}_b)$ and F is the feature semantics mapped from $(\mathbf{X}_f; \mathbf{X}_b)$, it follows that a portion of each F_i (belonging to the foreground) is informative for target recognition, while another portion (belonging to the background) occupies the position that should belong to the target information. Therefore, the goal of backdoor adjustment should be to emphasize the foreground-related portions, and to suppress the background-related portions of F that are irrelevant and harmful to target recognition. In this way, the true causality between \mathbf{X}_f and \mathbf{Y} can be excavated. Formally, the backdoor adjustment based $do(\cdot)$ operation can be expressed as follows:

$$P(\mathbf{Y}|do(\mathbf{X}_f)) = \sum_{i=1}^n P(\mathbf{Y}|\mathbf{X}_f, F_i)P(F_i). \quad (1)$$

This equation presents a theoretical solution to eliminate background interference. In the following subsection, we will delve into the specifics of implementing the terms described in (1), and we will also detail our proposed

method guided by this theoretical solution.

3.2. Causal Interventional Regularizer

In this subsection, we embody the theoretical background interference elimination process as a causal interventional regularizer.

Before introducing the proposed method, we note that in conventional DL-based models, the functional implementation of $P(\mathbf{Y}|\mathbf{X}_f)$ is provided by a supervised learning process with the cross-entropy loss function, as follows:

$$P(\mathbf{Y}|\mathbf{X}_f) = - \sum_{k=1}^K \mathbb{I}(\mathbf{Y} == k) \log \frac{\exp c_k((\mathbf{X}_f; \mathbf{X}_b))}{\sum_{j=1}^K \exp c_j((\mathbf{X}_f; \mathbf{X}_b))} \quad (2)$$

where k represents the k th class, c is the mapping: $\mathbb{R}^{n_c} \rightarrow \mathbb{R}^K$ from the last network layer to the softmax classification layer, and j is the j th dimension of the prediction probability.

To embody the backdoor adjustment process described in (1), the first step is to provide detailed functional implementations for $P(\mathbf{Y}|\mathbf{X}_f, F_i)$ and $P(F_i)$. Considering that F_i contains portions belonging to both foreground and background, generating large weights for the foreground-related channels and small weights for the background-related channels of F_i is necessary. By re-weighting F_i based on these weights, we can effectively address the need for background interference elimination.

Based on the above analyses, when a weight vector $\alpha_i = [\alpha_{i,1}, \alpha_{i,2}, \dots, \alpha_{i,n_c}]^T$ is given, the functional implementation for the first term of (1) can be expressed as:

$$P(\mathbf{Y}|\mathbf{X}_f, F_i) = - \sum_{k=1}^K \mathbb{I}(\mathbf{Y} == k) \log \frac{\exp c_k(F_i \odot \alpha_i)}{\sum_{j=1}^K \exp c_j(F_i \odot \alpha_i)} \quad (3)$$

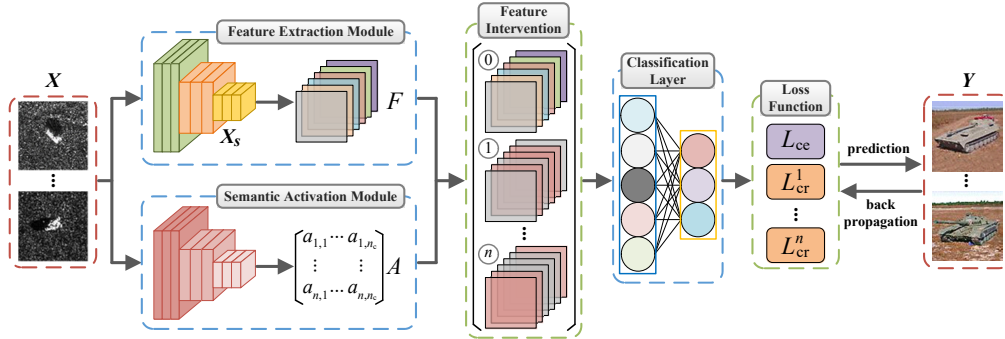


Figure 4: Illustration of the proposed causal intervention based regularization method. It is comprised of two modules, i.e., the feature extraction module and the semantic activation module. The former is a conventional DL-model for extracting the foreground and background features from the input SAR images. The latter can be seen as a causal interventional regularizer that is used to intervene on the obtained feature semantics, thus achieving the background debiased feature learning. In this figure, the instances and labels of training samples, network architectures, and intermediate outputs are marked by red, blue, and green boxes, respectively.

where $F_i \odot \alpha_i = [F_{i,1} \cdot \alpha_{i,1}, F_{i,2} \cdot \alpha_{i,2}, \dots, F_{i,n_c} \cdot \alpha_{i,n_c}]$. Therefore, given a weight matrix $A = [\alpha_1, \alpha_2, \dots, \alpha_n]$, and let $P(F_i) = 1/n$, the overall implementation of the backdoor adjustment based $do(\cdot)$ operation can be expressed as:

$$P(\mathbf{Y} | do(\mathbf{X}_f)) = - \sum_{i=1}^n \left(\sum_{k=1}^K \mathbb{I}(\mathbf{Y} == k) \log \frac{\exp c_k(F_i \odot \alpha_i) \times \frac{1}{n}}{\sum_{j=1}^K \exp c_j(F_i \odot \alpha_i)} \right). \quad (4)$$

The aforementioned approach shifts our focus from providing functional implementations for (1) to the task of generating the weight matrix A required in (4). To accomplish this, we use a learnable network to generate the required weight matrix. This idea inspires us to propose a novel regularization method with plug-and-play capability based on causal intervention. The DL-model that incorporates the proposed causal interventional regularizer is

comprised of two modules, i.e., the feature extraction module and the semantic activation module. The unified framework for this approach is depicted in Fig. 4. In the following, we give detailed descriptions of the two modules and the functional learning objective.

3.2.1. Feature Extraction Module

When integrating the proposed method with DL-based SAR-ATR models, a conventional DL-based feature extractor is utilized as the backbone to extract *task-specific features* from the SAR images containing both foreground and background. Therefore, the backbone of this module corresponds to \mathbf{X}_s in Fig. 3, while its output corresponds to the feature semantics of $(\mathbf{X}_f; \mathbf{X}_b)$.

We denote the training set as $D_{\text{train}} = \{X^i, Y^i\}_{i=1}^{i=N}$, where $X^i \in \mathbb{R}^{w \times h \times c}$ represents the instance with a size of $w \times h \times c$, and $Y^i \in \mathbb{R}$ represents the label in this set. The forward propagation of the feature extraction module can be expressed as $f_{\text{sem}}(X^i)$, where $f_{\text{sem}}(\cdot)$ is the mapping of the backbone of this module, parameterized by W_{sem} . It is used to map the input to the semantic space, i.e., $f_{\text{sem}} : \mathbb{R}^{w \times h \times c} \mapsto \mathbb{R}^{n \times n_c}$.

The proposed method has a plug-and-play capability, as we do not impose any restrictions on the feature extractor. This is evident from the definition of $f_{\text{sem}}(\cdot)$, allowing any DL-model to be used to build the feature extraction module.

3.2.2. Semantic Activation Module

After obtaining the preliminary feature semantics F using the feature extraction module, another backbone is utilized by this module to extract the *semantic-activation-specific features* and generate the weight matrix in

(4). Subsequently, the process of re-weighting from the preliminary to the background debiased feature semantics, i.e., $F_i \odot \alpha_i$, can be performed by intervening the feature semantics.

The forward propagation of the semantic activation module can be expressed as $f_{\text{sem}}(X^i) \odot f_{\text{sam}}(X^i)$, where $f_{\text{sam}}(\cdot)$ is the mapping of the backbone of this module, parameterized by W_{sam} . It is used to map the input to the semantic activation space, i.e., $f_{\text{sam}} : \mathbb{R}^{w \times h \times c} \mapsto \mathbb{R}^{n \times n_c}$, which activates the feature semantics belonging to the foreground while suppressing those belonging to the background, thereby excavating the true causality.

3.2.3. Overall Learning Objective

The classification layer, parameterized by W_{cls} , is used to map the preliminary and background debiased feature semantics to prediction probabilities. Then the forward prediction and loss back-propagation of our proposed framework can be supported. Following the definitions in (2) to (4), for the training set D_{train} , the learning objective for the feature extraction module can be expressed as the following cross-entropy loss:

$$L_{\text{ce}}(X, Y, W_{\text{sem}}, W_{\text{cls}}) = -\frac{1}{N} \sum_{i=1}^N \sum_{k=1}^K \mathbb{I}(Y^i == k) \log \frac{\exp c_k(f_{\text{sem}}(X^i))}{\sum_{j=1}^K \exp c_j(f_{\text{sem}}(X^i))}. \quad (5)$$

Besides, the t th learning objective for the semantic activation module can be expressed as the following causal interventional regularizer loss:

$$L_{\text{cr}}^t(X, Y, W_{\text{sem}}, W_{\text{sam}}, W_{\text{cls}}) = -\frac{1}{N} \sum_{i=1}^N \sum_{k=1}^K \mathbb{I}(Y^i == k) \log \frac{\exp c_k(f_{\text{sem}}^t(X^i) \odot f_{\text{sam}}^t(X^i)) \times \frac{1}{n}}{\sum_{j=1}^K \exp c_j(f_{\text{sem}}^t(X^i) \odot f_{\text{sam}}^t(X^i))}, \quad (6)$$

and the overall learning objective for this module is the sum of n times calculation for (6). Based on (5) and (6), we can obtain the overall learning objective of the unified framework shown in Fig. 4:

$$L_{\text{total}} = L_{\text{ce}} + \lambda \sum_{t=1}^n L_{\text{cr}}^t \quad (7)$$

where λ is the hyperparameter to control the trade-off. The two terms of (7) correspond to the $P(\mathbf{Y}|\mathbf{X}_f)$ and $P(\mathbf{Y}|do(\mathbf{X}_f))$ in the theoretical causal analysis, which reflects the integration of the conventional DL-model with our proposed causal interventional regularizer.

It is important to note that in a conventional DL-based SAR-ATR model, the loss function only includes the L_{ce} term. Therefore, the proposed method can be seen as a way to regularize the conventional model using the causal inference induced L_{cr} term. That is why we refer to the proposed method as *causal interventional regularizer* in this paper.

The training process of the proposed method is outlined as Algorithm 1.

4. Experiments

In this section, we first introduce the dataset used in the experiments. Then we proceed to demonstrate the performance of both the proposed method and the compared methods. Finally, we analyze the effect of the hyperparameter in the proposed method on its target recognition performance.

4.1. MSTAR Dataset

The experimental data utilized in this paper is obtained through the employment of the Sandia National Laboratory SAR sensor platform. This ven-

Algorithm 1 Training the Background Debiased SAR-ATR Model

Input:

Model parameter initialization W_{sem} , W_{sam} , and W_{cls} ;

Epoch I ;

Mini-batch size B ;

Learning rate η ;

Hyperparameter λ ;

Training and validation sets D_{train} and D_{val} .

- 1: **for** epoch in I : **do**
- 2: **for** batch in B : **do**
- 3: Forward propagation by f_{sem} , f_{sam} , and c with trainable parameters
 of W_{sem} , W_{sam} , and W_{cls}
- 4: # update the classification layer
- 5: $W_{\text{cls}} \leftarrow W_{\text{cls}} - \eta \nabla_{W_{\text{cls}}} L_{\text{total}}$
- 6: # update the semantic activation module
- 7: $W_{\text{sam}} \leftarrow W_{\text{sam}} - \eta \nabla_{W_{\text{sam}}} L_{\text{total}}$
- 8: # update the feature extraction module
- 9: $W_{\text{sem}} \leftarrow W_{\text{sem}} - \eta \nabla_{W_{\text{sem}}} L_{\text{total}}$
- 10: **end for**
- 11: **end for**

Return:

The DL-model with the highest validation accuracy.

ture received funding from the Defense Advanced Research Projects Agency and the Air Force Research Laboratory, as an integral component of the MSTAR program (AFRL and DARPA, 2020). The dataset released to the public comprise ten distinct ground target classes, namely armored personnel carrier types BMP-2, BRDM-2, BTR-60, and BTR-70; tanks T-62 and T-72; rocket launcher 2S1; air defense unit ZSU-234; truck ZIL-131; and bulldozer D7. The data is collected using an X-band SAR sensor, in a spotlight mode with a resolution of 1-ft and full aspect coverage (spanning 0° to 360°).

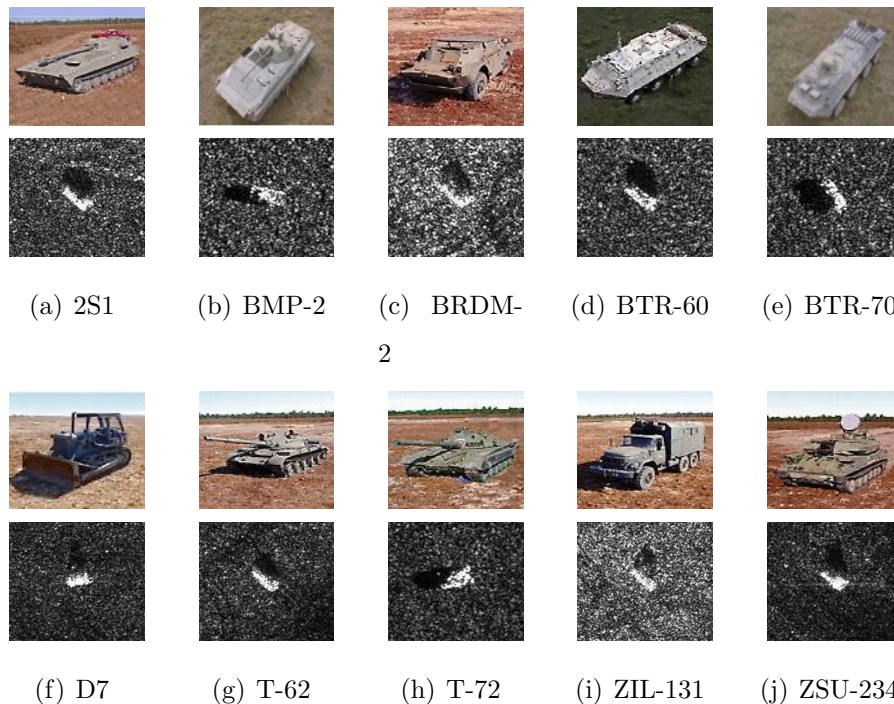


Figure 5: Ten types of military targets in the MSTAR dataset in the optical and SAR formats. (a) 2S1. (b) BMP-2. (c) BRDM-2. (d) BTR-60. (e) BTR-70. (f) D7. (g) T-62. (h) T-72. (i) ZIL-131. (j) ZUS-234.

The MSTAR benchmark dataset is widely employed for evaluating the

performance of SAR-ATR methods. Fig. 5 illustrates the SAR images of ten target classes contained in the MSTAR dataset, captured at similar aspect angles. In addition, it displays their corresponding optical images. In our experiments, involved SAR-ATR methods are thoroughly evaluated under standard operating conditions (SOC) as well as extended operating conditions (EOC) to ensure their appropriate evaluation. SOC primarily includes utilizing serial numbers and target configurations in the testing set that align with those in the training set, however, with varying aspects and depression angles. On the other hand, EOC involves substantial differences between the training and testing sets, highlighting notable variations in depression angle, target articulation, and version variants.

4.2. Experimental Settings

The effectiveness of the proposed method is demonstrated through comparisons with notable alternatives, including VGG16 (Simonyan and Zisserman, 2014), ResNet18 (He et al., 2016), and A-ConvNet (Chen et al., 2016). The former two are the predominant DL-models utilized in image recognition, whereas A-ConvNet holds extensive application in SAR-ATR domain.

In the experiments, we use a VGG16 model as the backbone of the semantic activation module. The patch size of input images is limited to 128×128 . The size of obtained feature map from backbone is $4 \times 4 \times 512$. When integrating the proposed method with the comparison methods, they will be used as the feature extractor in the feature extraction module in the proposed framework, and a fully-connected layer is attached behind them to generate the feature semantics.

Sophisticated data pre-processing and augmentation techniques are fre-

quently employed in related studies for better recognition performance. Nevertheless, to illustrate the inherent target recognition proficiency of the DL-models, we refrain from carrying out any pre-processing activities, such as de-speckle, on the SAR images to be recognized in the experimental setup. Furthermore, to accentuate the background debias capability of the proposed method, we do not perform any data augmentation for VGG16 and ResNet18 models, but retain the original data augmentation operation of A-ConvNet, which involves randomly sampling a substantial quantity of 88×88 patches from the original 128×128 SAR images. This data augmentation method aims to mitigate the negative impact of background on the feature learning of targets. The aforementioned settings facilitate a straightforward comparison between the effectiveness of the proposed and the data augmentation methods for the issue of background debias.

The mini-batch stochastic gradient descent based method is used for model optimization, with a batch size of 64, and a training epoch of 100. In order to accelerate the optimization process and obtain more precise approximate solutions, the Adam optimizer is employed with the learning rate of 0.01. Upon completion of the training process, the model with the highest validation accuracy is preserved.

The experiments of this study employ a NVIDIA RTX A6000 GPU, and the program is implemented using the PyTorch DL framework.

4.3. Experiments under SOC

In the experimental setup of SOC, which is listed in Table 1, the involved methods are evaluated on the ten-class recognition problem.

It must be noted that the target serial number is identical in both the

Table 1: Number of Training and Testing samples for the SOC Experimental Setup

Class	Training Set (17°)	Testing Set (15°)
2S1	299	274
BMP-2	233	196
BRDM-2	298	274
BTR-60	256	195
BTR-70	233	196
D7	299	274
T-62	299	273
T-72	232	196
ZIL-131	299	274
ZIL-234	299	274

Table 2: The comparison of Recognition Accuracy (%) under SOC

	CNN	VGG16	ResNet18	A-ConvNet
Accuracy(%)	91.483	92.783	95.685	98.376
	CNN+Ours	VGG16+Ours	ResNet18+Ours	A-ConvNet+Ours
	95.637	98.557	98.215	99.228

training and testing sets, although they vary in their azimuth and depression

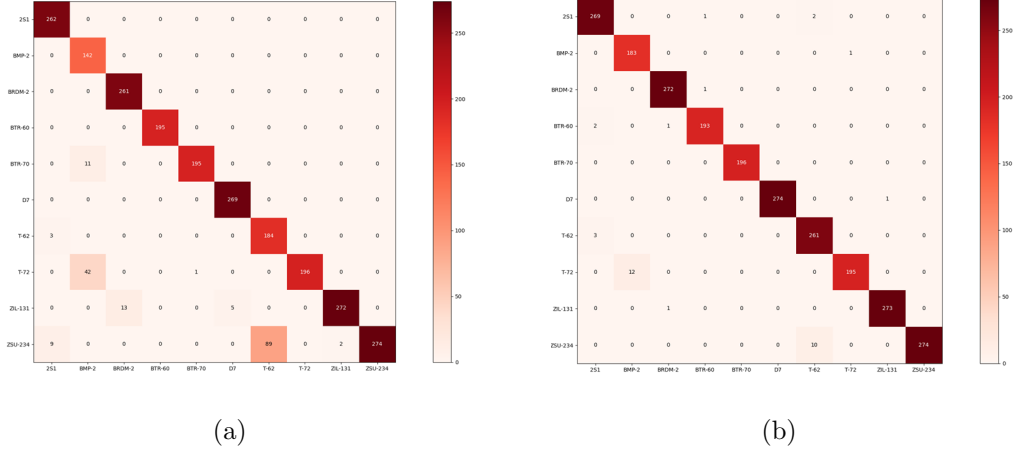


Figure 6: The comparison of confusion matrices under SOC. (a) Results of VGG16. (b) Results of background debiased VGG16.

angles. The training images are acquired at a depression angle of 17° , whereas the testing images are captured with a depression angle of 15° .

Table 2 shows the comparison of the testing accuracy of CNN, VGG16, ResNet18, A-Convnet before and after adding the proposed causal interventional regularizer. In addition, the comparison of confusion matrices before and after background debias for the VGG16 model is shown in Fig. 6.

As can be seen from the experimental results, for the three DL-models without data augmentation, they also show significant improvements in the testing accuracy after adding the proposed causal interventional regularizer. Among them, background debiased VGG16 model even outperforms the A-ConvNet model, which expands the original training set 1681 times by a random clipping based data augmentation method. Specifically, after the causal-driven regularizer is inserted, the involved four DL-models have 4.154%, 5.774%, 2.530%, and 0.852% improvement in the recognition accu-

racy, respectively. The greatly improved SAR-ATR performance shows that even if there are many background areas in the ROI that interfere with target semantic learning, the conventional DL-based models can still effectively focus on the extraction of foreground information after adding the proposed causal interventional regularizer. This demonstrates the satisfactory background debiased capability of the proposed method. In addition, since the proposal is a plug-and-play method, there is no need to make any modifications to the original model, which greatly improves the generalizability of various DL-based recognition models in the field of SAR-ATR.

4.4. Experiments under EOC

It is widely acknowledged that SAR images are highly susceptible to variations in depression angles. Therefore, the robustness of SAR-ATR methods to the changes in depression angle is important. To this end, we assess the proposed method in terms of large depression angle changes (indicated by EOC-1).

Table 3: Details of EOC-1 Experimental Setup

Target Type		Training Set		Testing Set	
Class	Serial No.	Depression	No. Samples	Depression	No. Samples
2S1	B01	17°	299	30°	288
BRDM-2	E71	17°	298	30°	287
T-72	A64	17°	299	30°	288
ZSU-234	D08	17°	299	30°	288

Table 3 enumerates that among the targets in the MSTAR dataset, only four classes (2S1, BRDM-2, T-72, and ZSU-234) possess targets obtained at a depression angle of 30° . Consequently, we evaluate the involved DL-models on these samples, wherein the corresponding training set is the data of these four classes of targets in SOC, i.e., the same targets obtained at a depression angle of 17° . The large disparity in depression angle may result in a dissimilar depiction of same targets in identical postures, thereby augmenting the difficulty of recognition.

The EOC-1 dataset is classified using two models: the conventional VGG16 model and the VGG16 model incorporating the proposed causal interventional regularizer. The confusion matrix for large depression angle variations is presented in Fig. 7. The experimental results indicate that the VGG16 model achieves the accuracy of 96.351% while our proposed model has a higher accuracy of 98.436%. This suggests that the proposed method is capable of improving the robustness of DL-based SAR-ATR models even under challenging conditions such as large depression angles.

In another EOC testing scenario, i.e., EOC-2, the assessment of SAR-ATR methods revolves around variations in target configuration. The objective of this validation is to evaluate the performance of the model to recognize different variants of the same target. Specifically, the training set encompasses BMP-2, BRDM-2, BTR-70 and T-72 at depression angles of 15° and 17° , whereas the testing set comprises of diversified versions of T-72. The variance in target representation between the two sets makes it arduous for the testing samples to be recognized as T-72 targets, thus intensifying the task challenge. Details of EOC-2 experimental setup are shown in Table 4.

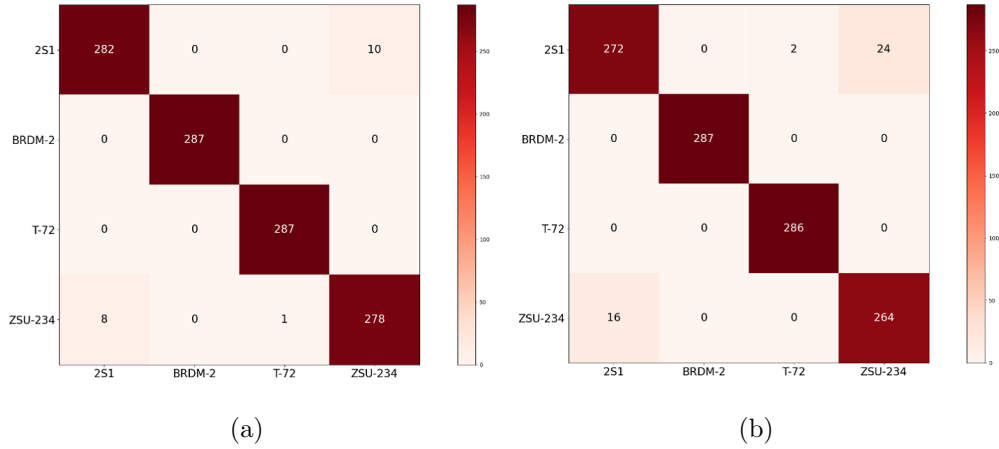


Figure 7: The comparison of confusion matrices under EOC-1. (a) Results of VGG16. (b) Results of background debiased VGG16.

Table 4: Details of EOC-2 Experimental Setup

Partition	Class	Serial No.	Depression	No. Samples
Training Set	BMP-2	C21	17°	233
	BRDM-2	E71	17°	298
	BTR-70	C71	17°	233
	T-72	132	17°	232
Testing Set	T-72	S7	15°/17°	419
		A32	15°/17°	572
		A62	15°/17°	573
		A63	15°/17°	573
		A64	15°/17°	573

Experimental results under EOC-2 can be seen from Table 5. Similar to the previous experiments, we choose VGG16 as a representative of the conventional DL-models to test its change in recognition accuracy before and after the addition of the proposed causal interventional regularizer.

Table 5: The comparison of Recognition Accuracy (%) under EOC-2

Serial No.	No. Samples	VGG16	VGG16+Ours
A32	572	88.462	95.979
A62	573	95.637	97.906
A63	573	94.939	96.684
A64	573	92.845	95.637
S7	419	79.714	80.191
Total	2710	90.923	94.022

It is relatively obvious from the experimental results that the incorporation of the proposed method improves the accuracy of the conventional DL-model for the recognition of all variant classes of T-72. In particular, the recognition accuracy of the serial number A32 is improved by 7.517%, which is a considerable improvement. The above results effectively verify the effectiveness of the proposed method for background debias when recognizing variants of the same target.

4.5. Hyperparameter Analysis

To comprehensively investigate the impact of hyperparameter on the SAR-ATR accuracy of the proposed method, we employ the VGG16 model with the proposed regularization method and conduct experiments under SOC. Our primary focus is on assessing the significance of the hyperparameter λ in (7) on recognition accuracy while moderating the proportion of the causal interventional regularizer induced loss L_{cr} in the overall loss L_{total} , which denotes the intervention degree of the proposed method in the feature extraction of conventional DL-model. We achieve this goal by setting the value of λ to $\{0.001, 0.01, 0.1, 0.5, 1.0\}$ and conduct comparative experiments. The results are presented in Fig. 8.

As demonstrated in Fig. 8, the selection of hyperparameter λ is critical in promoting a desirable background debias effect. Notably, the highest accuracy is attainable when λ is set to 0.1; deviating from this value, whether by setting it too high or low, can result in a significant decrease in recognition accuracy.

5. Conclusion

In this paper, we present the first attempt to investigate the potential of background debias on DL-based SAR-ATR models from a methodological perspective. Specifically, we propose a novel causal intervention based regularization method to eliminate the interference of background on the extraction of target semantic information. The proposed method is developed based on the analysis of the SAR-ATR oriented SCM, which depicts the causal relationships among the input, DL-model, foreground, background,

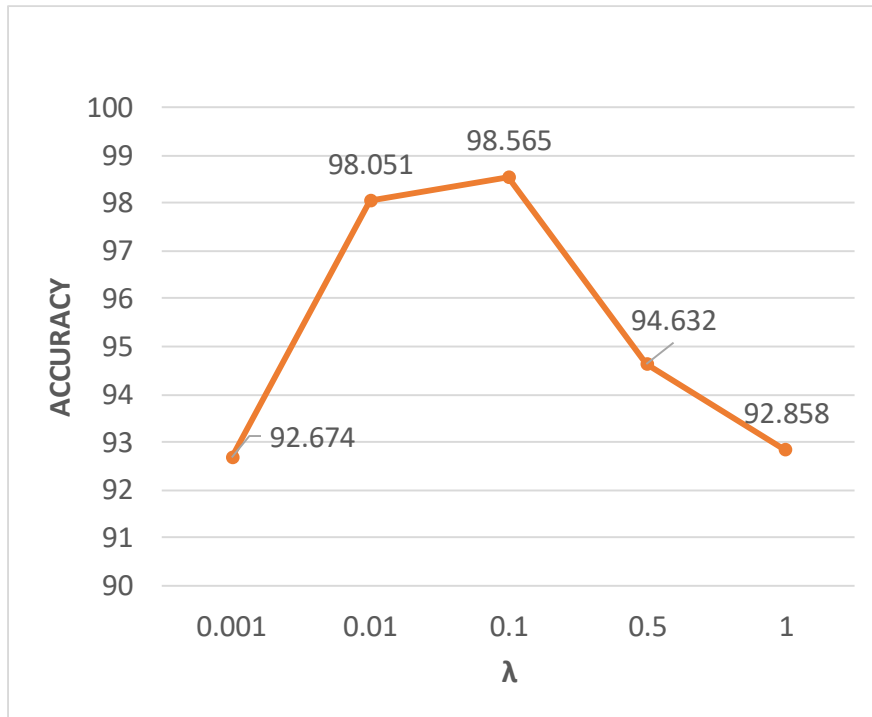


Figure 8: The effect of hyperparameter λ on the recognition accuracy.

and prediction.

We model the background in the SAR image to be recognized as a confounder for the feature extraction of DL-models, and eliminate it through backdoor adjustment based causal intervention. This theoretical solution for eliminating background interference is then transformed into a regularization term for conventional DL-models, resulting in background debiased feature learning. This method extracts more target semantics and improves the discriminability of the extracted features, while also being easy to implement, low complexity, widely adaptable, and having plug-and-play capability.

Experiments on the MSTAR dataset demonstrate that our proposed method

offers advantages over conventional approaches, as evidenced by improved recognition performance when combined with any conventional DL-model. Moving forward, we plan to explore the combination of causal inference and diverse tasks such as SAR target detection and change detection. We will also explore other learning pipelines, including self-supervised learning, few-shot learning, and model compression.

CRedit authorship contribution statement

H.D. and F.H. were responsible for the conceptualization, design and development of the methods, writing programmes, running experiments, analyzing the results, and writing the paper. L.S., W.Q. and L.Z. were responsible for investigation, funding requests and supervision. All authors reviewed the manuscript.

Conflict of interest

The authors declare that they have no conflict of interest.

Acknowledgments

This work was supported in part by the National Natural Science Foundation of China (62271172), in part by the China Postdoctoral Science Foundation (2023M733615).

References

References

- AFRL, DARPA, 2020. Sensor data management system website, MSTAR database. <https://www.sdms.afrl.af.mil/index.php?collection=mstar>.
- Amrani, M., Jiang, F., Xu, Y., Liu, S., Zhang, S., 2018. SAR-oriented visual saliency model and directed acyclic graph support vector metric based target classification. *IEEE J. Sel. Topics Appl. Earth Observ. Remote Sens.* 11, 3794–3810.
- Belloni, C., Balleri, A., Aouf, N., Le Caillec, J.M., Merlet, T., 2020. Explainability of deep SAR ATR through feature analysis. *IEEE Trans. Aerosp. Electron. Syst.* 57, 659–673.
- Chen, S., Wang, H., Xu, F., Jin, Y.Q., 2016. Target classification using the deep convolutional networks for SAR images. *IEEE Trans. Geosci. Remote Sens.* 54, 4806–4817.
- Cui, J., Gudnason, J., Brookes, M., 2005. Automatic recognition of MSTAR targets using radar shadow and superresolution features, in: *Proc. IEEE Int. Conf. Acoust., Speech, Signal Process. (ICASSP)*, pp. 589–589.
- Ding, J., Chen, B., Liu, H., Huang, M., 2016. Convolutional neural network with data augmentation for SAR target recognition. *IEEE Geosci. Remote Sens. Lett.* 13, 364–368.
- Du, C., Zhang, L., 2021. Adversarial attack for SAR target recognition based on UNet-generative adversarial network. *Remote Sens.* 13.

- El-Darymli, K., Gill, E.W., McGuire, P., Power, D., Moloney, C., 2016. Automatic target recognition in synthetic aperture radar imagery: A state-of-the-art review. *IEEE Access* 4, 6014–6058.
- El-Darymli, K., McGuire, P., Power, D., Moloney, C., 2013. Target detection in synthetic aperture radar imagery: A state-of-the-art survey. *J. Appl. Remote. Sens.* 7, 071598.
- Feng, S., Ji, K., Ma, X., Zhang, L., Kuang, G., 2022. Target region segmentation in SAR vehicle chip image with ACM net. *IEEE Geosci. Remote Sens. Lett.* 19, 4014605.
- Fu, K., Zhang, T., Zhang, Y., Wang, Z., Sun, X., 2022. Few-shot SAR target classification via metalearning. *IEEE Trans. Geosci. Remote Sens.* 60, 2000314.
- Glymour, M., Pearl, J., Jewell, N.P., 2016. *Causal inference in statistics: A primer.* John Wiley & Sons, Inc., Hoboken, NJ, USA.
- He, K., Zhang, X., Ren, S., Sun, J., 2016. Deep residual learning for image recognition, in: *Proc. IEEE Conf. Comput. Vis. Pattern Recognit. (CVPR)*, pp. 770–778.
- Huang, L., Liu, B., Li, B., Guo, W., Yu, W., Zhang, Z., Yu, W., 2018. Open-SARShip: A dataset dedicated to Sentinel-1 ship interpretation. *IEEE J. Sel. Topics Appl. Earth Observ. Remote Sens.* 11, 195–208.
- Kechagias-Stamatis, O., Aouf, N., 2021. Automatic target recognition on synthetic aperture radar imagery: A survey. *IEEE Aerosp. Electron. Syst. Mag.* 36, 56–81.

- Krizhevsky, A., Sutskever, I., Hinton, G.E., 2012. Imagenet classification with deep convolutional neural networks, in: Proc. Adv. Neural Inf. Process. Syst. (NIPS), pp. 1097–1105.
- Kwak, Y., Song, W.J., Kim, S.E., 2019. Speckle-noise-invariant convolutional neural network for SAR target recognition. *IEEE Geosci. Remote Sens. Lett.* 16, 549–553.
- LeCun, Y., Bengio, Y., Hinton, G.E., 2015. Deep learning. *Nature* 521, 436–444.
- LeCun, Y., Boser, B., Denker, J., Henderson, D., Howard, R., Hubbard, W., Jackel, L., 1989. Backpropagation applied to handwritten zip code recognition. *Neural Comput.* 1, 541–551.
- Lei, P., Zheng, T., Wang, J., Bai, X., 2021. A joint convolutional neural network for simultaneous despeckling and classification of SAR targets. *IEEE Geosci. Remote Sens. Lett.* 18, 1610–1614.
- Li, T., Du, L., 2019. SAR automatic target recognition based on attribute scattering center model and discriminative dictionary learning. *IEEE Sens. J.* 19, 4598–4611.
- Lombardo, P., Sciotti, M., Kaplan, L.M., 2001. SAR prescreening using both target and shadow information, in: Proc. IEEE Radar Conf. (RadarConf), pp. 147–152.
- Van der Maaten, L., Hinton, G.E., 2008. Visualizing data using t-SNE. *J. Mach. Learn. Res.* 9, 2579–2605.

- Moreira, A., Prats-Iraola, P., Younis, M., Krieger, G., Hajnsek, I., Papathanassiou, K.P., 2013. A tutorial on synthetic aperture radar. *IEEE Geosci. Remote Sens. Mag.* 1, 6–43.
- Papson, S., Narayanan, R.M., 2012. Classification via the shadow region in SAR imagery. *IEEE Trans. Aerosp. Electron. Syst.* 48, 969–980.
- Pearl, J., 2009. *Causality*. Cambridge University Press, Cambridge, UK.
- Pei, J., Huang, Y., Huo, W., Zhang, Y., Yang, J., Yeo, T.S., 2017. SAR automatic target recognition based on multiview deep learning framework. *IEEE Trans. Geosci. Remote Sens.* 56, 2196–2210.
- Peng, B., Peng, B., Zhou, J., Xie, J., Liu, L., 2022. Scattering model guided adversarial examples for SAR target recognition: Attack and defense. *IEEE Trans. Geosci. Remote Sens.* 60, 5236217.
- Ren, H., Yu, X., Zou, L., Zhou, Y., Wang, X., Bruzzone, L., 2021. Extended convolutional capsule network with application on SAR automatic target recognition. *Signal Process.* 183, 108021.
- Schölkopf, B., 2022. *Causality for Machine Learning*. Association for Computing Machinery, New York, NY, USA.
- Simonyan, K., Zisserman, A., 2014. Very deep convolutional networks for large-scale image recognition. *arXiv preprint arXiv:1409.1556* .
- Sun, X., Lv, Y., Wang, Z., Fu, K., 2022. SCAN: Scattering characteristics analysis network for few-shot aircraft classification in high-resolution SAR images. *IEEE Trans. Geosci. Remote Sens.* 60, 5226517.

- Sun, Y., Wang, Y., Liu, H., Wang, N., Wang, J., 2019. SAR target recognition with limited training data based on angular rotation generative network. *IEEE Geosci. Remote Sens. Lett.* 17, 1928–1932.
- Wang, C., Huang, Y., Liu, X., Pei, J., Zhang, Y., Yang, J., 2022. Global in local: A convolutional transformer for SAR ATR FSL. *IEEE Geosci. Remote Sens. Lett.* 19, 4509605.
- Wang, Z., Du, L., Li, Y., 2021. Boosting lightweight CNNs through network pruning and knowledge distillation for SAR target recognition. *IEEE J. Sel. Topics Appl. Earth Observ. Remote Sens.* 14, 8386–8397.
- Wen, Z., Liu, Z., Zhang, S., Pan, Q., 2021. Rotation awareness based self-supervised learning for SAR target recognition with limited training samples. *IEEE Trans. Image Process.* 30, 7266–7279.
- Zhang, M., An, J., Yang, L.D., Wu, L., Lu, X.Q., et al., 2020. Convolutional neural network with attention mechanism for SAR automatic target recognition. *IEEE Geosci. Remote Sens. Lett.* 19, 4004205.
- Zhang, X., Wang, Y., Li, D., Tan, Z., Liu, S., 2018. Fusion of multifeature low-rank representation for synthetic aperture radar target configuration recognition. *IEEE Geosci. Remote Sens. Lett.* 15, 1402–1406.
- Zhou, B., Khosla, A., Lapedriza, A., Oliva, A., Torralba, A., 2016. Learning deep features for discriminative localization, in: *Proc. IEEE Conf. Comput. Vis. Pattern Recognit. (CVPR)*, pp. 2921–2929.
- Zhou, Y., Chen, T., Tian, J., Zhou, Z., Wang, C., Yang, X., Shi, J., 2019. Complex background SAR target recognition based on convolution neural

network, in: Proc. IEEE 6th Asia-Pacific Conf. Synthetic Aperture Radar (AP SAR), pp. 1–4.

Zhu, X.X., Montazeri, S., Ali, M., Hua, Y., Wang, Y., Mou, L., Shi, Y., Xu, F., Bamler, R., 2021. Deep learning meets SAR: Concepts, models, pitfalls, and perspectives. *IEEE Geosci. Remote Sens. Mag.* 9, 143–172.

Zou, B., Qin, J., Zhang, L., 2022. Vehicle detection based on semantic-context enhancement for high-resolution SAR images in complex background. *IEEE Geosci. Remote Sens. Lett.* 19, 4503905.